

## Two-frequency acousto-optic modulator driver to improve the beam pointing stability during intensity ramps

B. Fröhlich, T. Lahaye, B. Kaltenhäuser, H. Kübler, S. Müller, T. Koch, M. Fattori, and T. Pfau

*5. Physikalisches Institut, Universität Stuttgart, Pfaffenwaldring 57, 70569 Stuttgart, Germany*

(Received 16 January 2007; accepted 1 March 2007; published online 2 April 2007)

We report on a scheme to improve the pointing stability of the first order beam diffracted by an acousto-optic modulator (AOM). Due to thermal effects inside the crystal, the angular position of the beam can change by as much as 1 mrad when the radio-frequency power in the AOM is reduced to decrease the first order beam intensity. This is done, for example, to perform forced evaporative cooling in ultracold atom experiments using far-off-resonant optical traps. We solve this problem by driving the AOM with two radio frequencies  $f_1$  and  $f_2$ . The power of  $f_2$  is adjusted relative to the power of  $f_1$  to keep the total power constant. Using this, the beam displacement is decreased by a factor of 20. The method is simple to implement in existing experimental setups, without any modification of the optics. © 2007 American Institute of Physics. [DOI: 10.1063/1.2720725]

### I. INTRODUCTION

An important application of acousto-optic modulators (AOMs) is the control of laser beam intensities. The power of the sound wave traveling inside the acousto-optic crystal determines the amount of light that is diffracted out of an incoming laser beam. However, thermal effects lead to a displacement of the diffracted beams when the power of the radio frequency (rf) driving the AOM is changed. The position stability is a critical parameter in many applications using AOMs, especially for dipole traps formed by strongly focused, far-off-resonant laser beams.<sup>1</sup> Such traps play a major role in atomic physics nowadays, as they allow for the realization of new experiments, for example, the Bose-Einstein condensation (BEC) of atomic species that cannot be condensed in magnetic traps such as cesium or chromium,<sup>2</sup> or the all-optical generation of a BEC.<sup>3</sup> Particularly in crossed optical dipole traps, where two beams have to be overlapped on a 10  $\mu\text{m}$  scale, a small change of the beam position can have a dramatic effect on the trap characteristics (frequency and depth), thus causing severe problems.<sup>4</sup> One way to circumvent them is to use a single-mode optical fiber after the AOM, but this cannot be done for high power lasers, such as CO<sub>2</sub> or ytterbium fiber lasers. Another option consists in changing the frequency of the rf to compensate for the beam movement. In this article, we report on a simpler scheme, adaptable to any AOM, which strongly reduces the beam displacement. The method is based on driving the AOM with two different radio frequencies,  $f_1$  and  $f_2$ , and adjusting their relative powers,  $P_1$  and  $P_2$ , so that the total rf power,  $P = P_1 + P_2$ , in the AOM is kept constant.<sup>5</sup> This article is organized as follows: After describing the experimental setup with which we measure the beam displacement, we present our measurements for AOMs in the 1 and 10  $\mu\text{m}$  wavelength range. In an Appendix, we show the details of the electronic circuit we used to adjust  $P_2$  relative to  $P_1$  with a single control voltage.

### II. EXPERIMENTAL SETUP

We test the two-frequency method with two AOM models that use different acousto-optic crystals to modulate the light. The setup for measuring the beam displacement of the first AOM using a tellurium dioxide (TeO<sub>2</sub>) crystal (Crystal Technology 3110-199) is shown in Fig. 1. We use an ytterbium fiber laser (IPG, model YLR-20-1064-LPSF) at 1064 nm, with 10 W output power. The  $1/e^2$  beam radius is reduced with a telescope from 2.1 to 0.7 mm before going through the AOM. After the AOM, a beam block stops all the light except the beam used, which is attenuated and monitored with a charge-coupled device (CCD) camera. We fitted the images with a two-dimensional (2D) Gaussian and recorded the peak position of the beam profile. The setup for the second AOM using a germanium (Ge) crystal (IntraAction Corp. AGM-406B1) is slightly different. We use a CO<sub>2</sub> laser (Coherent GEM100L) at 10.6  $\mu\text{m}$ , with 21 W of power going through the AOM. At a distance of about 3 m, we measure the beam profile in one dimension with a movable pinhole in front of a power meter. We fitted the profile with a Gaussian and recorded the peak position.

Figure 2 shows the modified AOM driver that one has to use for the two-frequency method. To control laser intensities with an AOM, one has to change the rf power driving it. This

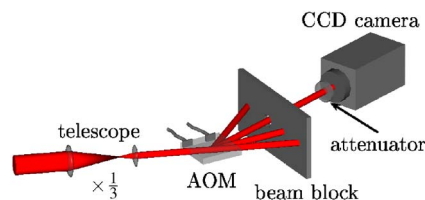


FIG. 1. (Color online) Setup for measuring the beam displacement of the AOM using a TeO<sub>2</sub> crystal. The size of the laser beam is reduced with a telescope before it enters the AOM. A beam block after the AOM stops all light except the beam used, which is attenuated and monitored with a CCD camera. The distance between the AOM and the camera is 1.4 m.

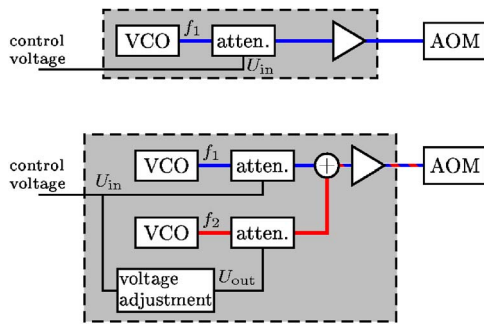


FIG. 2. (Color online) (a) Normal setup for driving an AOM with variable rf power. A voltage controlled oscillator (VCO) generates the radio frequency  $f_1$  (blue line), which is attenuated to a value given by the control voltage  $U_{in}$ . The signal is then amplified before going to the AOM. (b) For the two-frequency AOM driver, we add an extra VCO and attenuator. The additional VCO generates the second rf signal  $f_2$  (red line), whose power is adjusted relative to  $f_1$  to keep the total power in the AOM constant. This adjustment is done by modifying the control voltage  $U_{in}$  with an electronic circuit (shown in detail in the Appendix). For the TeO<sub>2</sub> AOM, we use the following Mini-Circuits components: VCO POS-150, attenuator PAS-3, combiner ZMSC-2-1, and amplifier ZHL-1-2W.

can be done by attenuating a rf signal coming from a voltage controlled oscillator (VCO) before amplifying it to its final value [Fig. 2(a)]. The amount of light that is diffracted out of the incoming beam is then determined by the control voltage  $U_{in}$ . For the two-frequency driver, we add a second VCO and attenuator [Fig. 2(b)] with frequency  $f_2$ . The two frequencies  $f_1$  and  $f_2$  are chosen close enough in order to be well within the bandwidth of the AOM,<sup>6</sup> but far enough to give a sufficient separation of the two first order beams. We use  $f_1 = 99$  MHz (30 MHz) and  $f_2 = 123$  MHz (50 MHz) for the TeO<sub>2</sub> (Ge) AOM. The power of frequency  $f_2$  generated by the second VCO is adjusted relative to the power of  $f_1$  in order to keep the total power in the AOM constant. To do this with a single control voltage,  $U_{in}$  is modified by an electronic circuit (see Appendix) before it is applied to the second attenuator. We adjust the transfer function  $U_{out}(U_{in})$  of the circuit to have a constant total rf power after the signals are added *and amplified*; the latter condition being crucial to take into account the amplifier saturation.

Laser light going through an AOM driven by two frequencies is diffracted in many different beams as can be seen in Fig. 3. The image was taken with the TeO<sub>2</sub> AOM at about equal power of both rf signals. Besides the zeroth order beam, the first order beam of both frequencies, as well as second and even third order beams, which correspond to

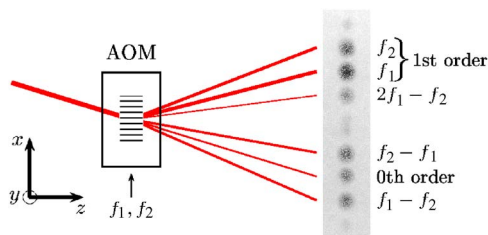


FIG. 3. (Color online) Schematic of the AOM driven by two frequencies. The image shows a picture of the laser beam diffracted by the TeO<sub>2</sub> AOM. On the right hand side of the image, the frequency shifts corresponding to the diffracted light are indicated ( $f_1 = 99$  MHz and  $f_2 = 123$  MHz).

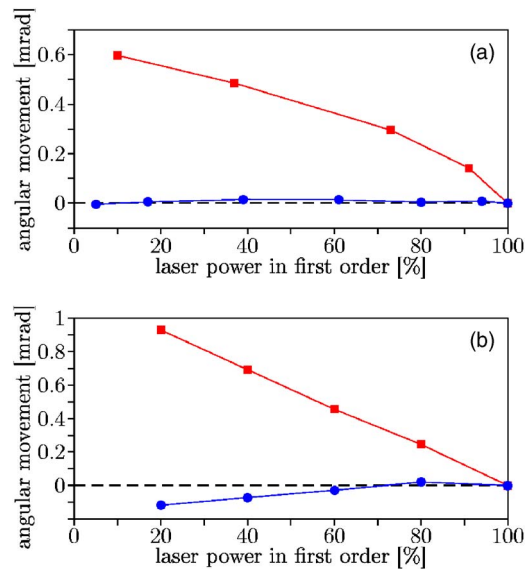


FIG. 4. (Color online) (a) Measured angular movement of the first order beam perpendicular to the plane of diffraction ( $y$ ) with (blue circles) and without the second frequency (red squares) for the TeO<sub>2</sub> AOM. The movement is plotted as a function of the relative laser power in the first order with respect to its maximum value. (b) Same measurement for the Ge AOM, measured in the diffraction plane  $x$ .

multiple absorption and stimulated emission of phonons,<sup>7</sup> can be seen. To measure the beam displacement, we optimize the angle between the acoustic wave and the incident laser beam to have the maximum power in the first order of  $f_1$ . With full power at this frequency and none at  $f_2$ , we achieve diffraction efficiencies up to 90%.

### III. MEASUREMENTS

With the setups described above we measure the position of the first order beam of  $f_1$  at different rf powers for the two AOMs, with and without the second frequency. In Fig. 4 we plot the angular movement as a function of the laser power in the first order beam. Figure 4(a) shows the displacement perpendicular to the plane of diffraction  $y$  for the TeO<sub>2</sub> AOM. The displacement in the plane of diffraction  $x$  (not shown in the figure) has the same dependence as that perpendicular to it, but is smaller by a factor of 3. Adding the second fre-

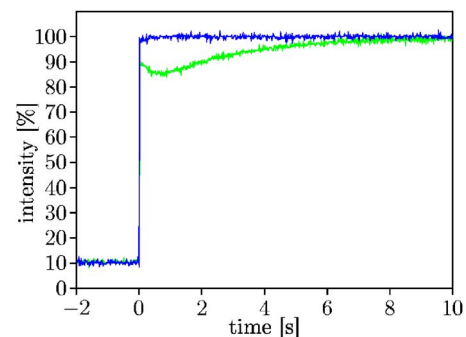


FIG. 5. (Color online) Time dependence of the laser intensity when switching the rf power rapidly. Without the second frequency (green), it takes nearly 10 s for the intensity to stabilize to its steady state value. With the second frequency (blue), there is only a very small transient effect during the first second after switching.

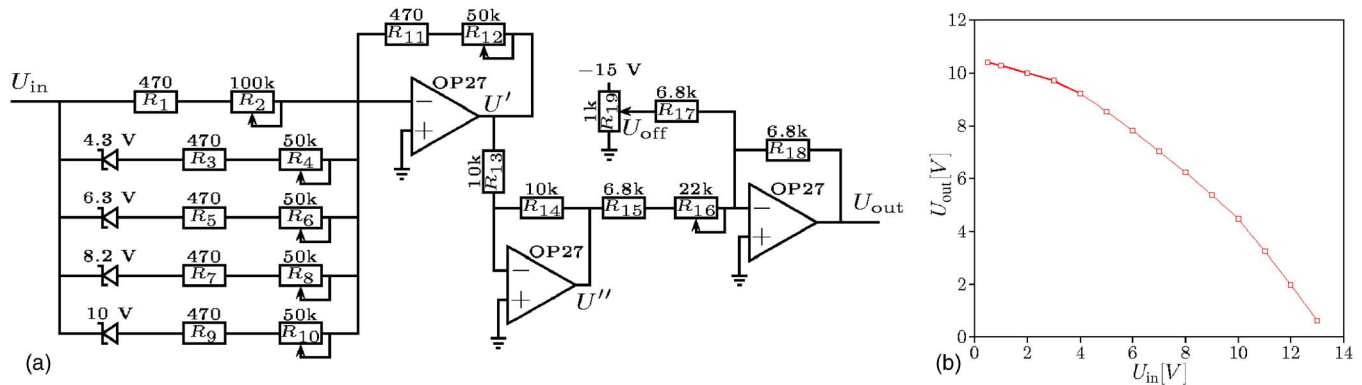


FIG. 6. (Color online) (a) Schematic of the electronic circuit for adjusting the control voltage. The gain of the first inverting amplifier depends on the voltage  $U_{in}$  due to the Zener diodes. The amplified voltage is inverted again before a variable offset  $U_{off}$  is added in the last step. (b) Measured transfer function of the circuit.

quency keeps the beam position almost constant (below 0.03 mrad), whereas without, a beam displacement of up to 0.6 mrad occurs. A big improvement is also evident for the Ge AOM [Fig. 4(b)], where the angular movement is reduced by a factor of 10. The fact that we are not able to compensate the displacement as well as with the TeO<sub>2</sub> AOM is due to the higher rf power that the AOM is driven with. For maximum diffraction efficiency, the Ge AOM needs 30 W rf power, whereas the TeO<sub>2</sub> AOM needs only 2 W. Another TeO<sub>2</sub> AOM that we tested (A-A Opto-Electronics deflector, model MTS80-A3-1064Ac) uses a sheer mode acoustic wave and needs only 0.5 W rf power for maximum diffraction efficiency. Its beam movement is significantly smaller than for the other AOMs, only up to 0.1 mrad, but still larger than for the two-frequency method.<sup>8</sup>

To supplement those steady state measurements, we have also checked for the TeO<sub>2</sub> crystal that the suppression of the beam movement remains good when the rf power is *dynamically* ramped down over a time scale of a few seconds, as is done for forced evaporative cooling of ultracold atoms.

The two-frequency method helps also to stabilize the laser power  $P$  in the first order when switching the rf power rapidly, as can be seen in Fig. 5, which shows the time dependence of  $P(t)$  for the TeO<sub>2</sub> AOM. Without the second frequency, it takes about 10 s to reach the steady state value when switching the laser power abruptly from 10% to 100%. The beam displacement takes place over the same time scale. Only a very small transient effect can be seen during the first second after switching when using the two-frequency method.

In conclusion we have demonstrated a simple method to improve the pointing stability of a beam diffracted by an AOM when the intensity is ramped down. The salient advantage of this technique lies in the fact that only the rf driver has to be modified, without any modifications of the optics.

## ACKNOWLEDGMENTS

The authors thank C. S. Adams for useful discussions and W. Möhrle for the design of the digital control box. The authors gratefully acknowledge the support of the German Science Foundation (DFG) (SFB/TR 21) and the Landesstif-

tung Baden-Württemberg. One of the authors (T.L.) acknowledges support from the European Marie Curie Grant MEIF-CT-2006-038959.

## APPENDIX: VOLTAGE ADJUSTMENT CIRCUIT

In this Appendix we present a simple way to realize the voltage adjustment needed for the two-frequency method [Fig. 2(b)]. The electronic circuit shown in Fig. 6(a) modifies the control voltage  $U_{in}$ , so that the total rf power stays constant in the AOM. We measured the required calibration curve  $U_{out}$  as a function of  $U_{in}$ , which the circuit approximates by a stepwise linear function. To do this, we use an inverting amplifier whose gain at low voltages is given by  $-(R_{11}+R_{12})/(R_1+R_2)$ . Parallel to  $R_1$  and  $R_2$  are other resistors ( $R_3, R_4, \dots$ ) in series with Zener diodes. If  $U_{in}$  is larger than the Zener voltage of one of the diodes, it becomes conducting and the gain is increased. For example, if  $4.3 \text{ V} \leq U_{in} \leq 6.3 \text{ V}$ , the gain is increased to  $(R_{11}+R_{12})/(R_1+R_2) \parallel (R_3+R_4)$ . Thus, each time  $U_{in}$  exceeds a Zener voltage of one of the diodes, the gain increases. The amplified voltage  $U'$  is then inverted to  $U''$  before (in the last step) the voltage  $U_{off}$  is added. The potentiometer  $R_{16}$  allows for an extra gain in the last step. We use large potentiometers for all resistors to have a big flexibility for the transfer function. In Fig. 6(b) the measured transfer function is plotted. With this, we are able to keep the total rf power constant within 10% after amplification, which is enough to strongly reduce the beam displacement. For the setup using the Ge AOM, we use a more complex control box, which digitizes  $U_{in}$  with an analog-to-digital converter and then generates the output voltage  $U_{out}$  according to a conversion table written in an erasable programmable read-only memory (EPROM).

<sup>1</sup>R. Grimm, M. Weidemüller, and Yu. B. Ovchinnikov, Adv. At., Mol., Opt. Phys. **42**, 95 (2000).

<sup>2</sup>T. Weber, J. Herbig, M. Mark, H.-C. Nägerl, and R. Grimm, Science **299**, 232 (2003); A. Griesmaier, J. Werner, S. Hensler, J. Stuhler, and T. Pfau, Phys. Rev. Lett. **94**, 160401 (2005).

<sup>3</sup>M. D. Barrett, J. A. Sauer, and M. S. Chapman, Phys. Rev. Lett. **87**, 010404 (2001).

<sup>4</sup>R. Dumke, M. Johanning, E. Gomez, J. D. Weinstein, K. M. Jones, and P. D. Lett, *New J. Phys.* **8**, 64 (2006).

<sup>5</sup>This method is mentioned briefly in M. E. Gehm, Ph.D. thesis, Duke University, 2003.

<sup>6</sup>We obtain the AOM bandwidth by measuring the reflected power as a function of the radio frequency using a directional coupler (Mini-Circuits ZDC-10-1).

<sup>7</sup>D. L. Hecht, *IEEE Trans. Sonics Ultrason.* **SU-24**, 7 (1977).

<sup>8</sup>One drawback of the acousto-optic deflector is that the sound velocity for the shear mode in  $\text{TeO}_2$  is significantly smaller (by a factor of 5) than for the longitudinal mode, leading to longer rise times. Using the two-frequency method with a longitudinal mode AOM allows one to keep fast rise times.